THE EUROPEAN
PHYSICAL JOURNAL C

Ellis wormholes in anti-de Sitter space

Jose Luis Blázquez-Salcedo[1,a], **Xiao Yan Chew**[2,3,b] , **Jutta Kunz**[4,c] , **Dong-han Yeom**[2,3,d]

[1] Departamento de Fśica Teórica and IPARCOS, Universidad Complutense de Madrid, 28040 Madrid, Spain
[2] Department of Physics Education, Pusan National University, Busan 46241, Republic of Korea
[3] Research Center for Dielectric and Advanced Matter Physics, Pusan National University, Busan 46241, Republic of Korea
[4] Institut für Physik, Universität Oldenburg, Postfach 2503, 26111 Oldenburg, Germany

Abstract We construct traversable wormholes with anti-de Sitter asymptotics supported by a phantom field. These wormholes are massless and symmetric with respect to reflection of the radial coordinate $\eta \to -\eta$. Their circumferential radius decreases monotonically from radial infinity to their single throat. Analogous to their asymptotically flat counterparts, these anti-de Sitter wormholes possess an unstable radial mode.

1 Introduction

Wormholes represent intriguing solutions of the gravitational field equations that feature a minimal surface which is known as their throat, connecting distant regions in the universe. In general relativity (GR), the Einstein–Rosen (ER) bridge is probably the most well-known example of a non-traversable wormhole. It can be naturally obtained from the Schwarzschild black hole by maximally extending the solution [1]. On the other hand, in order to obtain traversable wormholes, a violation of the null energy condition is necessary. In GR this is typically accomplished by the introduction of some form of exotic matter (see, e.g., [2–4]).

Here the static asymptotically flat Ellis wormholes [5–7] represent the classic example of traversable wormholes. They are supported by a phantom field, which corresponds to a scalar field with an opposite sign of the kinetic term, thus violating the null energy condition. Such a phantom field can be used to describe the accelerated expansion of the universe [8–11] and can also be employed to construct black holes [12,13], four-dimensional black rings [14], or star-like objects [15].

Static Ellis wormholes have a very simple geometric structure. They possess a single throat that connects two asymptotically flat regions. They have been generalized to higher dimensions [16], and to include rotation in four dimensions [17–20] and five dimensions [21]. Also, configurations of wormholes with phantom fields and ordinary fields have been constructed as, for example, Ellis wormholes immersed in bosonic matter [22–25] or mixed neutron star-wormhole systems [26–30].

Whereas static Ellis wormholes possess an unstable radial mode in both four and higher dimensions [16,31–34], the inclusion of rotation might stabilize these wormholes, as suggested by a study of rotating wormholes with equal angular momenta in five dimensions [21]. Here, at the onset of rotation, a zero mode turns into a second unstable radial mode, which bifurcates with the first unstable mode at a critical value of the angular momentum, leaving sufficiently rapidly rotating wormholes without unstable radial modes.

However, the presence of a phantom field is not mandatory to obtain traversable wormholes. Numerous such wormholes have been obtained in alternative theories of gravity, when the energy conditions have been violated in the gravitational sector (see, e.g., [35–45]). But even in GR, wormholes can be supported only by fermions [46], i.e., the constituents of ordinary matter, which is also sufficient to violate the energy conditions. In particular, traversable wormholes of Einstein–Maxwell–Dirac theory have recently been constructed [47].

From an astrophysical perspective, wormholes might mimic black holes (see e.g. [48,49]). Here, in order to distinguish them from black holes, a number of astrophysical signatures of wormholes have been pointed out that might allow us to search for their existence in the near future. Examples are their shadows [50–52], gravitational lensing [53–59], accretion disks around wormholes [60,61], and their ringdown phase with the associated emission of gravitational waves [62].

[a] e-mail: jlblaz01@ucm.es

[b] e-mail: xychew998@gmail.com (corresponding author)

[c] e-mail: jutta.kunz@uni-oldenburg.de

[d] e-mail: innocent.yeom@gmail.com

On the other hand, there has been much interest in recent years regarding wormholes that connect asymptotically locally anti-de Sitter (AdS) spaces; indeed, such wormholes have been constructed in a variety of gravitational models [63–70]. However, the generalization of asymptotically flat Ellis wormholes to AdS asymptotics has not yet been explored. Hence, in this paper we close this gap and construct Ellis wormholes with a negative cosmological constant. We then investigate the properties of these wormholes and explore how the AdS asymptotics affects the stability of the solutions.

This paper is organized as follows. In Sect. 2, we briefly introduce our theoretical setup comprising the phantom field and the metric ansatz. In addition, we derive the set of coupled differential equations, we describe the numerical methods employed to solve these equations, and we study the asymptotic behavior of the metric functions. In particular, we discuss the mass of the wormholes in asymptotically AdS spacetimes and the geometric properties of the wormholes, as well as the violation of the energy conditions. In Sect. 3, we present and discuss our numerical results for the wormhole solutions. In Sect. 4, we study the stability of the wormholes by calculating the unstable mode of the radial perturbations of the metric and the phantom field. Finally, in Sect. 5, we summarize our work and present an outlook.

2 Theoretical setting

2.1 Theory

We consider the Einstein–Hilbert action including the cosmological constant Λ and the Lagrangian for the matter field $\mathscr{L}_m$

$$S_{\mathrm{EH}} = \int \mathrm{d}^4 x \sqrt{-g} \left[\frac{1}{16\pi G}(R - 2\Lambda) + \mathscr{L}_{\mathrm{ph}} \right], \quad (1)$$

where Λ is related to the AdS length l by $\Lambda = -3/l^2$, and $\mathscr{L}_{\mathrm{ph}}$ is the Lagrangian of the phantom field ψ,

$$\mathscr{L}_{\mathrm{ph}} = \frac{1}{2} \partial_\mu \psi \, \partial^\mu \psi. \quad (2)$$

By varying the action with respect to the metric, we obtain the Einstein equations

$$R_{\mu\nu} - \frac{1}{2} g_{\mu\nu} R + \Lambda g_{\mu\nu} = 2\kappa T_{\mu\nu}, \quad (3)$$

where $\kappa = 4\pi G$, and the stress–energy tensor $T_{\mu\nu}$ is given by

$$T_{\mu\nu} = \frac{1}{2} g_{\mu\nu} \partial_\alpha \psi \, \partial^\alpha \psi - \partial_\mu \psi \, \partial_\nu \psi. \quad (4)$$

We obtain the massless Klein–Gordon equation by varying with respect to the phantom field,

$$\frac{1}{\sqrt{-g}} \partial_\mu \left(\sqrt{-g} \partial^\mu \psi \right) = 0. \quad (5)$$

In order to construct wormhole solutions with AdS asymptotics, we employ the following line element with a quasi-isotropic radial coordinate η,

$$\mathrm{d}s^2 = -F(\eta)N(\eta)\mathrm{d}t^2 + \frac{p(\eta)}{F(\eta)}$$
$$\times \left[\frac{\mathrm{d}\eta^2}{N(\eta)} + h(\eta)(\mathrm{d}\theta^2 + \sin^2\theta \mathrm{d}\varphi^2) \right], \quad (6)$$

where $N(\eta) = 1 - \Lambda\eta^2/3$ and $h(\eta) = \eta^2 + \eta_0^2$, with η_0 the throat parameter. In pure Einstein gravity ($\Lambda = 0$), the above metric describes a static Ellis wormhole that possesses two asymptotically flat regions $\Sigma_\pm$ as $\eta \to \pm\infty$. The analytical solution for static Ellis wormholes is given by

$$p(\eta) = 1, \quad F(\eta) = e^{f(\eta)}, \quad (7)$$

with

$$f(\eta) = \frac{2M}{\eta_0} \left[\arctan\left(\frac{\eta}{\eta_0}\right) - \frac{\pi}{2} \right], \quad (8)$$

and M is the mass of the Ellis wormholes on Σ_+. However, when $\Lambda < 0$, the above metric should possess two asymptotically AdS regions as $\eta \to \pm\infty$.

2.2 Ordinary differential equations (ODEs)

By substituting the line element Eq. (6) into the Einstein equations, we obtain a set of second-order nonlinear ODEs for the metric functions,

$$F'' - \frac{F}{p}p'' + \left[\frac{p'}{2p} + \frac{\eta(6N - h\Lambda)}{3hN} \right]F'$$
$$- \frac{\eta F(6N - h\Lambda)}{3phN}p' + \frac{3F}{4p^2}p'^2 - \frac{5}{4F}F'^2$$
$$- \frac{6hFN + 3\Lambda ph^2 - 2h\Lambda\eta^2 F - 3hF - 3\eta^2 FN}{3Nh^2}$$
$$= -\kappa F\psi'^2, \quad (9)$$

$$\frac{\Lambda\eta}{3FN}F' + \frac{\eta(3N - h\Lambda)}{3phN}p' + \frac{p'^2}{4p^2} - \frac{F'^2}{4F^2}$$
$$+ \frac{3N\eta^2 F + 3\Lambda ph^2 - 3hF - 2h\Lambda\eta^2 F}{3Fh^2 N}$$
$$= -\kappa\psi'^2, \quad (10)$$

$$p'' + \frac{\eta(3N - h\Lambda)}{3hN}p' - \frac{2\Lambda\eta p}{3FN}F' - \frac{p'^2}{p} + \frac{p}{2F^2}F'^2$$
$$+ \frac{2p(3hFN - 2h\Lambda\eta^2 F + 3\Lambda ph^2 - Fh^2\Lambda - 3\eta^2 FN)}{3FNh^2}$$
$$= 2\kappa p\psi'^2, \quad (11)$$

where the prime denotes the derivative of the functions with respect to the radial coordinate η.

From the massless Klein–Gordon equation Eq. (5) for the phantom field we obtain a first integral,

$$\psi' = \frac{D}{hN\sqrt{p}}, \tag{12}$$

where D is a constant. In the asymptotically flat case it is interpreted as the scalar charge of the phantom field. We eliminate the term ψ'^2 in Eqs. (9) and (11) by adding Eqs. (9) and (11), respectively, to Eq. (10). Then we obtain the following ODEs for the metric functions F and p,

$$F'' = \frac{F'^2}{F} + \frac{\Lambda\eta F}{3pN}p' - \left(\frac{p'}{2p} + \frac{2\eta(3N - h\Lambda)}{3hN}\right)F'$$
$$+ \frac{2\Lambda(2\eta^2 F + Fh - 3ph)}{3Nh}, \tag{13}$$

$$p'' = \frac{p'^2}{2p} - \frac{\eta(3N - h\Lambda)}{Nh}p'$$
$$+ \frac{2p(3F - 3FN + 4\Lambda\eta^2 F + \Lambda hF - 6\Lambda ph)}{3hFN}. \tag{14}$$

In order to study the asymptotic behavior of the metric functions in the limit $\eta \to \infty$, we perform the series expansion for Eqs. (13) and (14) to obtain the asymptotic expansion for the functions

$$F(\eta) = F_\infty + \frac{F_\infty \eta_0^2}{3\eta^2} - \frac{F_\infty \eta_0^2 (\Lambda\eta_0^2 - 12)}{15\Lambda\eta^4} + O(\eta^{-6}), \tag{15}$$

$$p(\eta) = F_\infty - \frac{F_\infty \eta_0^2}{3\eta^2} + \frac{F_\infty \eta_0^2 (14\Lambda\eta_0^2 + 27)}{45\Lambda\eta^4} + O(\eta^{-6}). \tag{16}$$

We observe that the odd terms vanish identically. With these expansions, the large-η expansions of g_{tt} and $g^{\eta\eta}$ for the wormhole are given by

$$-g_{tt}\Big|_{\eta\to\infty} = -\frac{\Lambda F_\infty \eta^2}{3} + F_\infty\left(1 - \frac{\Lambda\eta_0^2}{9}\right)$$
$$+ \frac{F_\infty \eta_0^2}{15\eta^2}\left(1 + \frac{\Lambda\eta_0^2}{3}\right) + O(\eta^{-4}), \tag{17}$$

$$g^{\eta\eta}\Big|_{\eta\to\infty} = -\frac{\Lambda\eta^2}{3} + 1 - \frac{2\Lambda\eta_0^2}{9}$$
$$+ \frac{\eta_0^2(7\Lambda\eta_0^2 + 81)}{135\eta^2} + O(\eta^{-4}). \tag{18}$$

Since the odd terms vanish, we find that the metric functions at $\eta \to -\infty$ have exactly the same asymptotic expansions as the metric functions at $\eta \to \infty$. According to the asymptotic expansions, the appropriate boundary conditions to be imposed on the metric functions at infinity are given by

$$F(\pm\infty) = p(\pm\infty) = 1, \tag{19}$$

and thus $F_\infty = 1$.

Considering the expression for the mass of the wormholes as, for instance, obtained from the Ashtekar–Magnon–Das formalism [73–75], the vanishing of the odd terms also implies that the mass of these symmetric wormholes vanishes, as also happens in the symmetric case for an asymptotically flat space. Indeed, the mass is read off from a term of order $1/\eta$, which is not present in the above expansion. However, other symmetric wormholes depending only on $|\eta|$ may feature a term of order $1/|\eta|$ and therefore possess a finite mass (see, e.g., [71]). In addition, the series expansion at $\eta = 0$ is given by

$$F(\eta) = F_0 + \frac{\Lambda}{3}(F_0 - 3p_0)\eta^2 + O(\eta^4), \tag{20}$$

$$p(\eta) = p_0 + \frac{\Lambda p_0(F_0 - 6p_0)}{3F_0}\eta^2 + O(\eta^4). \tag{21}$$

By using Eq. (12), we may rewrite Eq. (10) as

$$D^2 = \frac{N^2 ph^2}{4F^2}F'^2 - \frac{Np\Lambda\eta h^2}{3F}F' - \frac{N^2 h^2}{4p}p'^2$$
$$- \frac{1}{3}N\eta h(3N - h\Lambda)p'$$
$$- \frac{Np(3N\eta^2 F + 3\Lambda ph^2 - 3Fh - 2h\Lambda\eta^2 F)}{3F}. \tag{22}$$

This equation can be used to monitor the accuracy of the numerical computation by ensuring that D is constant on the grid in the full domain of integration. We note that in GR without a cosmological constant, for a generic static Ellis wormhole, the mass M and the scalar charge D are related by

$$D^2 = M^2 + \eta_0^2. \tag{23}$$

We solve Eqs. (13) and (14) numerically by using the ODE solver package COLSYS, which tackles boundary value problems for systems of nonlinear coupled ODEs based on the Newton–Raphson method [72]. Employing an adaptive grid selection procedure and using more than 1000 points, COLSYS provides the solutions with high accuracy together with an error estimate. To integrate the ODEs in the full interval $-\infty$ to $+\infty$, we compactify the radial coordinate η in the numerical calculations as follows: $\eta = \eta_0 \tan(\pi x/2)$ with $x \in [-1, 1]$. Moreover, we change to dimensionless variables by introducing the following rescaled variables/parameters in the above ODEs,

$$\tilde{\psi} = \sqrt{\kappa}\psi, \quad \eta = \eta_0\tilde{\eta}, \quad \Lambda = \frac{\tilde{\Lambda}}{\eta_0^2}. \tag{24}$$

In the remaining sections we will omit the tilde for convenience. After the rescaling, the only free parameter left is Λ.

2.3 Geometric properties

To study the geometric properties of the wormholes, we now define the circumferential radius R_c as

$$R_c(\eta) = \sqrt{\frac{ph}{F}} \, . \tag{25}$$

A wormhole throat is a minimal surface of the wormhole. Therefore, it has to satisfy the following conditions,

$$\left.\frac{dR_c}{d\eta}\right|_{\eta=\eta_{th}} = 0 \, , \quad \left.\frac{d^2 R_c}{d\eta^2}\right|_{\eta=\eta_{th}} > 0 \, , \tag{26}$$

where η_{th} is the radial coordinate of the throat. If a wormhole has an equator with radial coordinate η_{eq}, this requires

$$\left.\frac{dR_c}{d\eta}\right|_{\eta=\eta_{eq}} = 0 \, , \quad \left.\frac{d^2 R_c}{d\eta^2}\right|_{\eta=\eta_{eq}} < 0 \, . \tag{27}$$

An equator is typically located between two throats, and thus signals a double-throat configuration.

A wormhole throat can be visualized by embedding the equatorial plane ($\theta = \pi/2$) in Euclidean space (ρ, φ, z). Using cylindrical coordinates, this implies for the above metric parametrization

$$ds^2 = \frac{p}{FN} d\eta^2 + \frac{ph}{F} d\phi^2 \tag{28}$$
$$= d\rho^2 + dz^2 + \rho^2 d\phi^2 \, . \tag{29}$$

We then obtain the expression for z by comparison,

$$z = \pm \int \sqrt{\frac{p}{FN} - \left(\frac{d\rho}{d\eta}\right)^2} \, d\eta \, , \quad \rho \equiv R_c \, , \tag{30}$$

where the sign of z depends on the sign of the radial coordinate η. For the special case of the massless symmetric Ellis wormhole without cosmological constant ($\Lambda = 0$, $F = p = 1$), this yields

$$z = \int_0^\eta \sqrt{1 - \frac{\eta'^2}{\eta'^2 + \eta_0'^2}} \, d\eta' = \operatorname{arcsinh}\left(\frac{\eta}{\eta_0}\right) \, . \tag{31}$$

2.4 Null energy condition (NEC)

As noted above, the construction of wormholes requires the violation of the energy conditions. Here, we focus on the NEC, which states that

$$T_{\mu\nu} k^\mu k^\nu \geq 0 \, , \tag{32}$$

for all (future-pointing) null vectors k_μ which satisfy $k_\mu k^\mu = 0$. We note that the violation of the NEC also implies the violation of the weak and strong energy conditions.

Since the wormhole spacetime is spherically symmetric, there are two choices of null vector [44],

$$k_\mu = \left(g_{tt}, \sqrt{-\frac{g_{tt}}{g_{\eta\eta}}}, 0, 0\right) \, , \quad \text{and}$$
$$k_\mu = \left(1, 0, \sqrt{-\frac{g_{tt}}{g_{\theta\theta}}}, 0\right) \, , \tag{33}$$

which yield two expressions to test NEC violation,

$$-T^t{}_t + T^\eta{}_\eta \geq 0 \, , \quad -T^t{}_t + T^\theta{}_\theta \geq 0 \, . \tag{34}$$

Evaluating the above expressions explicitly,

$$-T^t{}_t + T^\eta{}_\eta = -\frac{D^2 F}{p^2 h^2 N} < 0 \, , \quad -T^t{}_t + T^\theta{}_\theta = 0 \, , \tag{35}$$

shows that the NEC is always violated.

3 Results and discussion

We have systematically constructed asymptotically AdS wormhole solutions for values of the cosmological constant Λ in the range $-100 \leq \Lambda \leq 0$. These wormholes are symmetric with respect to $\eta \to -\eta$. In the limit $\Lambda \to 0$ the asymptotically flat Ellis wormhole is obtained, where $F = p = 1$. We illustrate our results in Figs. 1, 2 and 3.

The metric components g_{tt} and $g_{\eta\eta}$ are shown in Fig. 1a, b, respectively, for a set of values of the cosmological constant, including the asymptotically flat case (black). As Λ decreases from zero, the asymptotic behavior changes to AdS. This is reflected in the asymptotic $\sim \eta^2$ and $\sim \eta^{-2}$ dependence of g_{tt} and $g_{\eta\eta}$, respectively. The component g_{tt} has its global maximum at $\eta = 0$. As Λ decreases from zero, the global maximum of g_{tt} increases slightly from -1 to a maximal value, and then decreases with further decreasing Λ, as demonstrated in Fig. 1c.

The metric component $g_{\eta\eta}$ is shown in Fig. 1b. When Λ decreases from zero it develops a local minimum at $\eta = 0$. This local minimum is, however, surrounded symmetrically by two degenerate maxima. As Λ decreases further, the maxima move toward $\eta = 0$, until they merge with the minimum. Finally, a single maximum at $\eta = 0$ remains, which decreases in size with further decreasing Λ. Figure 1d shows the phantom field function $\psi(x)$ versus the compactified coordinate x for the same set of values of the cosmological constant as shown in Fig. 1a, b.

In Fig. 2 we address some properties of the asymptotically AdS wormhole solutions. In Fig. 2a we show the phantom field constant D^2 versus the cosmological constant Λ. When
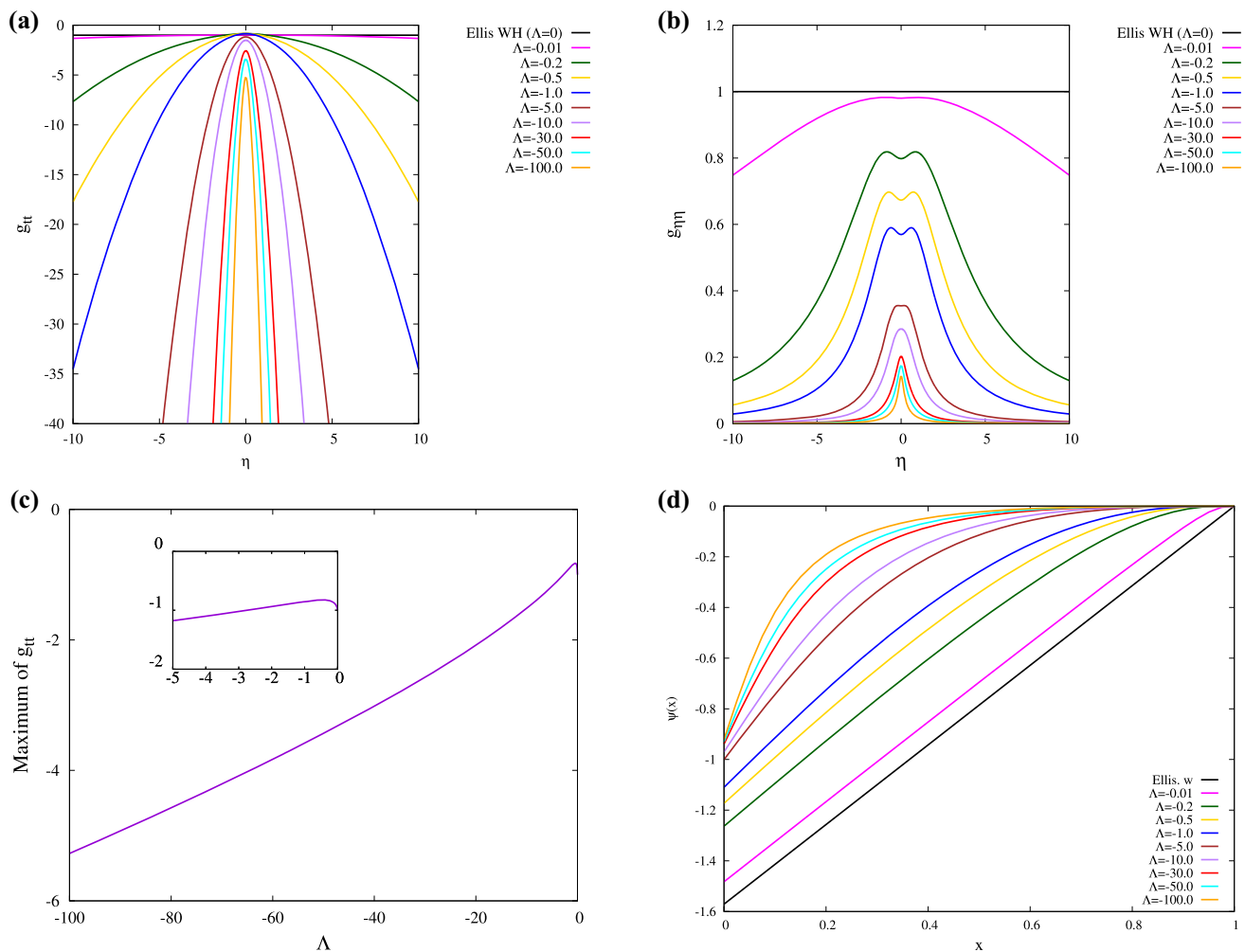
Fig. 1 Metric functions **a** g_{tt} and **b** $g_{\eta\eta}$ vs. the radial coordinate η for $-100 \le \Lambda \le 0$; **c** global maximum of g_{tt} vs. the cosmological constant Λ; **d** phantom field function $\psi(x)$ vs. the compactified coordinate x for $-100 \le \Lambda \le 0$

$\Lambda = 0$, D represents the phantom field charge, which is unity (given the scaling relations (24)) for a massless Ellis wormhole. With decreasing Λ, the constant D^2 at first decreases slightly to a minimum value, and then increases almost linearly as Λ decreases further.

Turning to the geometric properties of the wormholes, we show the circumferential radius R_c versus the radial coordinate η in Fig. 2b for several values of Λ. R_c has a single minimum at $\eta = 0$, from where it rises monotonically toward infinity on both sides. This minimum corresponds to the throat of the respective wormhole. Thus the wormholes possess a single throat.

The circumferential radius R_c of the throat is shown versus the cosmological constant in Fig. 2c. The throat radius is largest when $\Lambda = 0$, which corresponds to the Ellis wormhole. The throat radius decreases monotonically as Λ decreases. Note that the circumferential coordinate R_c tends to the modulus of the radial coordinate η.

The violation of the NEC as expressed via condition (35) is demonstrated in Fig. 2d. The violation is minimal when $\Lambda = 0$, and thus for the Ellis wormhole. The NEC violation increases significantly at the throat when Λ decreases.

The wormhole throat can be clearly visualized with the help of embedding diagrams as shown in Fig. 3. The figures also demonstrate that the size of the throat radius decreases as Λ decreases. (Note the change in the grid size.)

4 Linear stability

The investigation of the stability of wormholes is of considerable relevance. It is well known that the asymptotically flat static Ellis wormholes in GR possess an unstable radial mode [16,31,32]. Therefore, we will now address the stability of static Ellis wormholes with AdS asymptotics by studying radial perturbations on these new background solutions.
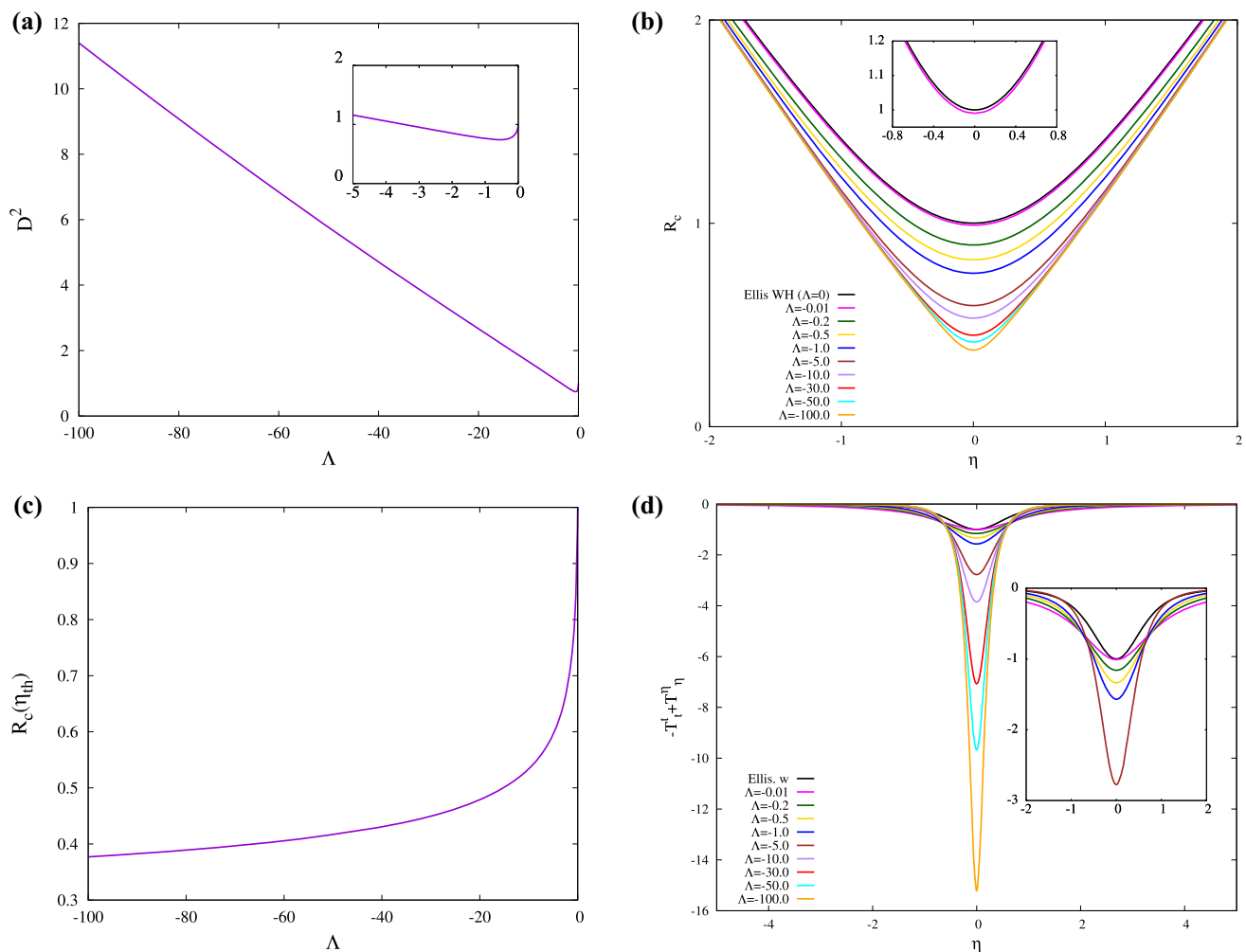
(a)

(b)

(c)

(d)

Fig. 2 Properties of wormhole solutions: **a** phantom field constant D^2 vs. Λ; **b** circumferential radius R_c vs. radial coordinate η for several values of Λ; **c** circumferential throat radius vs. Λ; **d** NEC violation vs. radial coordinate η for several values of Λ

We start by introducing the following ansatz for the line element

$$ds^2 = -e^{\nu(t,\eta)} N(\eta) dt^2 + e^{-\lambda(t,\eta)} \frac{p(\eta)}{N(\eta)} d\eta^2$$
$$+ p(\eta) h(\eta) e^{-\sigma(t,\eta)} (d\theta^2 + \sin^2\theta \, d\varphi^2), \qquad (36)$$

where

$$\nu(t,\eta) = \nu_0(\eta) + \epsilon \nu_1(\eta) e^{-i\omega t},$$
$$\lambda(t,\eta) = \lambda_0(\eta) + \epsilon \lambda_1(\eta) e^{-i\omega t},$$
$$\sigma(t,\eta) = \sigma_0(\eta) + \epsilon \sigma_1(\eta) e^{-i\omega t}, \qquad (37)$$

and the relation with the background metric is

$$e^{\nu_0} = e^{-\lambda_0} = e^{-\sigma_0} = F. \qquad (38)$$

For the phantom field we employ the ansatz

$$\Psi(t,\eta) = \psi(\eta) + \epsilon \Psi_1(\eta) e^{-i\omega t}. \qquad (39)$$

A mode with eigenvalue ω^2 is unstable and increases exponentially when $\omega^2 < 0$.

Inserting the Ansätze into the scalar field equation, we find

$$\Psi_1'' + \left(\frac{p'}{2p} + \frac{2\eta}{h} - \frac{2\Lambda\eta}{3N} \right) \Psi_1' + \omega^2 \frac{p\Psi_1}{F^2 N^2} = 0, \qquad (40)$$

when choosing the simple gauge-fixing

$$\lambda_1 = -\nu_1 + 2\sigma_1. \qquad (41)$$

Inserting the ansatz into the Einstein equations, we obtain the following set of first-order ODEs when again making use of the gauge-fixing (41)

$$\nu_1' = \frac{q_1}{6phNq_0} \nu_1 - \frac{q_2}{18phFN^2q_0} \sigma_1$$
$$- \frac{2DF(-6\eta pN - 3hNp' + 2\Lambda\eta ph)}{3h\sqrt{p}N^2q_0} \Psi_1 + \frac{4DF\sqrt{p}}{Nq_0} \Psi_1', \qquad (42)$$
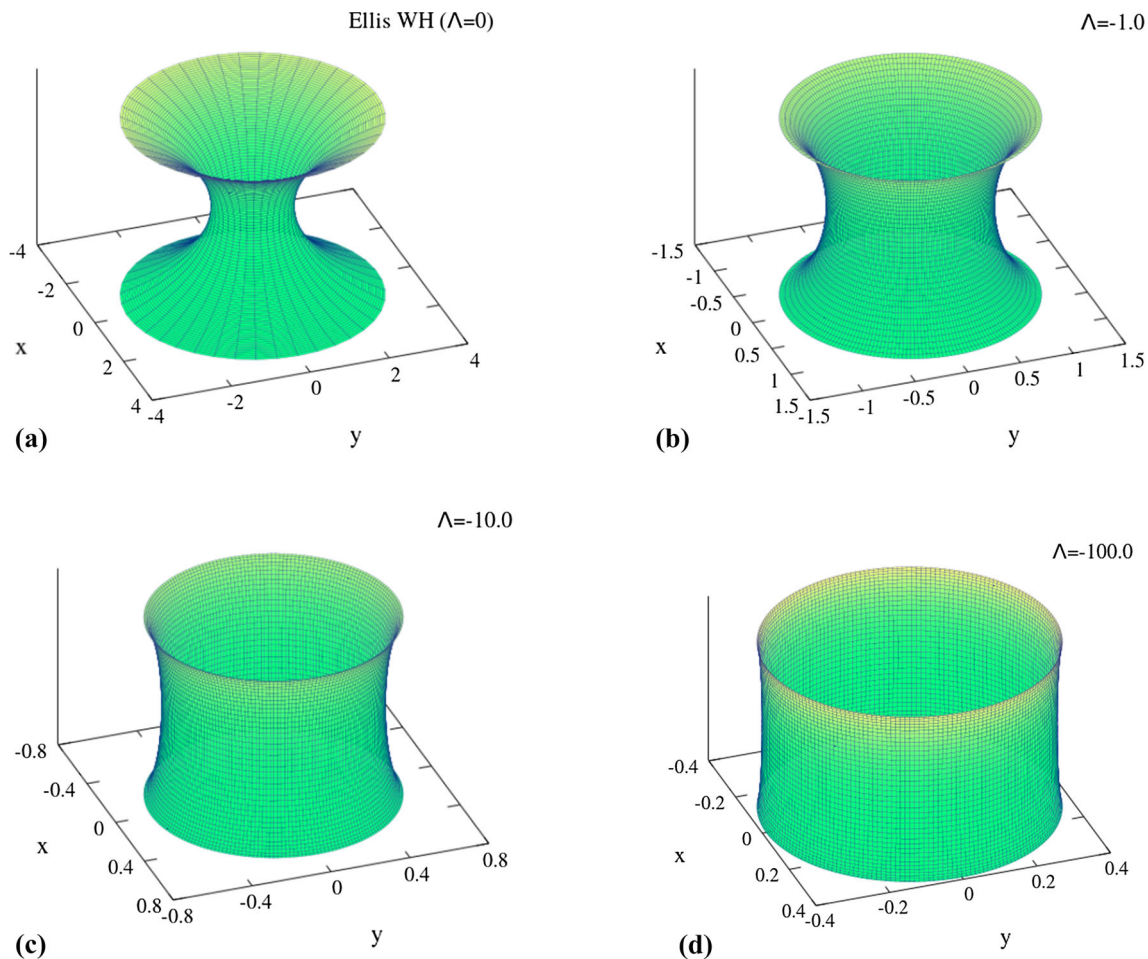
Fig. 3 Isometric embeddings of wormhole solutions for several values of Λ: **a** $\Lambda = 0.0$; **b** $\Lambda = -1.0$; **c** $\Lambda = -10.0$; **d** $\Lambda = -100.0$

$$\sigma_1' = \left(-\frac{p'}{2p} - \frac{\eta}{h} + \frac{F'}{2F} \right) v_1$$
$$+ \left(\frac{\eta}{h} - \frac{\Lambda\eta}{3N} + \frac{p'}{2p} \right) \sigma_1 - \frac{2D}{hN\sqrt{p}} \Psi_1, \tag{43}$$

where

$$q_0 = -2\eta pF - hFp' + phF', \tag{44}$$

$$q_1 = -12hFp^2 + 12\eta^2 p^2 FN + 3FNh^2 p'^2$$
$$+ 12\Lambda h^2 p^3 - 4\Lambda \eta^2 hFp^2 + 12\eta pNhFp'$$
$$- 3pNh^2 F'p' - 6\eta hNp^2 F'$$
$$+ 2\Lambda \eta p^2 h^2 F' - 2\Lambda \eta p Fh^2 p', \tag{45}$$

$$q_2 = 36\eta^2 p^2 F^2 N^2 + 9N^2 h^2 F^2 p'^2 - 36hNp^2 F^2$$
$$- 12\Lambda \eta p Nh^2 F^2 p' + 4\Lambda^2 \eta^2 p^2 h^2 F^2$$
$$+ 36p^3 h^2 \omega^2 + 36\eta hp F^2 N^2 p'$$
$$- 24\Lambda \eta^2 hNp^2 F^2 + 72\Lambda FNh^2 p^3. \tag{46}$$

We now first analyze Eq. (40) for the scalar field perturbation Ψ_1. By multiplying Eq. (40) by a factor $hN\sqrt{p}$ and making use of the product rule, we can combine the two

derivative terms on the left-hand side to obtain

$$\left(hN\sqrt{p}\Psi_1' \right)' + \omega^2 \frac{hp^{3/2}\Psi_1}{NF^2} = 0. \tag{47}$$

We then multiply the new ODE by Ψ_1, and integrate by parts over the full interval $(-\infty, \infty)$. Hence we obtain

$$\left(hN\sqrt{p}\Psi_1\Psi_1' \right)\Big|_{-\infty}^{\infty} = \int_{-\infty}^{\infty} h\sqrt{p} \left(N\Psi_1'^2 - \omega^2 \frac{p\Psi_1^2}{NF^2} \right) d\eta. \tag{48}$$

Since we require Ψ to be normalizable, the left-hand side of this equation vanishes. Therefore, the integral on the right-hand side must also vanish. However, the integrand is non-negative if an unstable mode ($\omega^2 < 0$) exists. Consequently, Ψ_1 has to be zero, so that the integral will vanish identically.

Next we consider Eqs. (42) and (43). They can be combined into a single master equation which is Schrödinger-like when written in terms of the perturbation function $Z = G_s\sigma_1$,

$$\frac{d^2Z}{dr_*^2} + (\omega^2 - V_R(\eta))Z = 0, \tag{49}$$

where r_* is the tortoise coordinate and $V_R(\eta)$ is the radial effective potential,

$$\frac{\mathrm{d}r_*}{\mathrm{d}\eta} = \frac{\sqrt{p}}{FN}, \quad V_R(\eta) = \frac{Q_1}{12h^2 p^3 Q_0}, \tag{50}$$

with

$$\begin{aligned}
\frac{1}{G_s}\frac{\mathrm{d}G_s}{\mathrm{d}\eta} = &-\frac{1}{2\eta^2 hpNFq_0} \\
&\times \left(-4\eta^3 hpNF^2 p' + 12FNh^2 p^3 - 12Fh^2 p^3 \right. \\
&-4\eta^4 Np^2 F^2 + 4\eta^2 hp^2 F^2 - N\eta^2 h^2 F^2 p'^2 \\
&\left.-\eta^2 Nh^2 p^2 F'^2 + 2\eta^2 pFNh^2 p'F' + 4\eta^3 hFNp^2 F'\right),
\end{aligned} \tag{51}$$

$$\begin{aligned}
Q_0 = &\ p^2 h^2 F'^2 - 4\eta hFp^2 F' - 2pFh^2 p'F' + 4\eta^2 p^2 F^2 \\
&+ 4\eta phF^2 p' + h^2 F^2 p'^2,
\end{aligned} \tag{52}$$

$$\begin{aligned}
Q_1 = &-48N^2\eta^4 p^4 F^4 - 3N^2 h^4 F^4 p'^4 + 96\Lambda^2 F^2 h^4 p^6 \\
&-192\Lambda h^3 F^3 p^5 + 144\eta^2 h^2 N^2 p^3 F^3 F' p' \\
&+72\eta p^2 N^2 h^3 F^3 F' p'^2 \\
&+48\eta\Lambda NF^3 h^3 p^4 p' - 72\eta F^2 N^2 h^3 p^3 p'F'^2 \\
&-3N^2 p^4 h^4 F'^4 + 36NF^2 h^3 p^4 F'^2 - 64\Lambda^2\eta^2 h^3 F^3 p^5 \\
&+64\Lambda\eta^2 h^2 p^4 F^4 - 12Np^2 h^3 F^4 p'^2 \\
&-48hN\eta^2 p^4 F^4 + 12pN^2 F^3 h^4 F' p'^3 \\
&-48\eta Nh^2 p^3 F^4 p' - 48\eta Nh^2 F^3 p^4 F' \\
&-24NF^3 h^3 p^3 p'F' + 32\eta\Lambda^2 F^2 h^4 p^5 F' \\
&-36\Lambda FNh^4 p^5 F'^2 - 32\eta\Lambda^2 F^3 p^4 h^4 p' \\
&-32\Lambda\eta F^3 h^3 p^4 F' + 32\Lambda\eta h^3 p^3 F^4 p' \\
&+12FN^2 p^3 h^4 p'F'^3 + 24\eta FN^2 h^3 p^4 F'^3 \\
&-72\eta^2 h^2 F^2 N^2 p^4 F'^2 \\
&+48\Lambda\eta^2 Nh^2 F^3 p^5 + 96hN^2\eta^3 F^3 p^4 F' \\
&-96hN^2\eta^3 p^3 F^4 p' - 72\eta^2 h^2 N^2 p^2 F^4 p'^2 \\
&+12\Lambda Nh^4 F^3 p^3 p'^2 \\
&-18p^2 N^2 F^2 h^4 p'^2 F'^2 - 24\eta pN^2 h^3 F^4 p'^3 \\
&+48\Lambda\eta NF^2 h^3 p^5 F' + 24\Lambda NF^2 h^4 p^4 F' p' \\
&+96h^2 p^4 F^4,
\end{aligned} \tag{53}$$

where we have used F'' and p'' to simplify the above expressions.

The radial effective potential is illustrated in Fig. 4a versus the compactified radial coordinate x for several values of the cosmological constant. It is symmetric with respect to $\eta \to -\eta$, exhibiting symmetric minima. The larger Λ is, the farther away from the throat are these minima of the potential.

Similarly to what happens in the asymptotically flat case, the potential diverges at the throat $\eta = 0$, as indicated in Fig. 4a. The analytical expansion of the potential around the throat shows that it diverges like η^{-2},

$$V_R(\eta) = \frac{2F_0^2}{p_0\eta^2} + O(\eta^0). \tag{54}$$

However, a difference with respect to the asymptotically flat case is that the potential also diverges at the two spatial infinities when the cosmological constant is not zero, as also indicated in Fig. 4a. The expansion of the potential at infinity shows that the potential diverges like η^2,

$$V_R(\eta) = \frac{2}{9}F_\infty\Lambda^2\eta^2 + O(\eta). \tag{55}$$

We compute the unstable mode numerically by using COLSYS to solve Eq. (49), which is an eigenvalue problem with ω^2 as the eigenvalue. In general, the perturbation function Z does not vanish at the infinities (this is the case because these are spherical perturbations of an asymptotically AdS configuration). However the perturbation equation requires that the derivative of the perturbation function vanishes at the boundaries, $\partial_\eta Z(-\infty) = \partial_\eta Z(\infty) = 0$. We impose these as boundary conditions. Since Eq. (49) is homogeneous, in order to obtain a nontrivial and normalizable solution for Z, we introduce an auxiliary equation $\frac{\mathrm{d}}{\mathrm{d}\eta}\omega^2 = 0$ that allows us to impose the condition $Z(\eta_p) = 1$ at some point η_p which we typically choose to be above the throat. The eigenvalue ω^2 is found when Z satisfies all the asymptotic boundary conditions. With this method, the estimated error of the modes reported in the following is typically 1% or smaller.

We present the eigenvalue ω^2 versus the cosmological constant in Fig. 4b. We show two different modes. In purple we show the unstable mode with $\omega^2 < 0$. This unstable mode is found for any value of the cosmological constant, and in particular, as $\Lambda \to 0$, it tends to the value of the unstable mode for the asymptotically flat massless Ellis solution (as seen in the inset). Hence, we conclude that the change of asymptotics does not stabilize the wormhole, since the unstable mode of the asymptotically flat solution can be continued smoothly for arbitrary values of the cosmological constant. In fact, note that the larger the magnitude of the cosmological constant (i.e., the shorter the AdS length), the larger the absolute value of the unstable mode becomes.

In this figure we also show in green a nodeless normal mode with $\omega^2 > 0$. This mode corresponds to stable perturbations. Because of the AdS asymptotics, gravitational waves are reflected by the conformal boundary, acting in practice like a box. This is different from the asymptotically flat case, where the perturbations oscillate while being damped exponentially in time (quasinormal modes). With AdS asymptotics, however, the oscillation is not damped, but reflected at the boundaries, and it is possible to find normal modes like the one we include in the figure. Note that the frequency grows as we decrease the AdS length. And in the limit $\Lambda \to 0$, it vanishes with $\omega^2 = 0$.
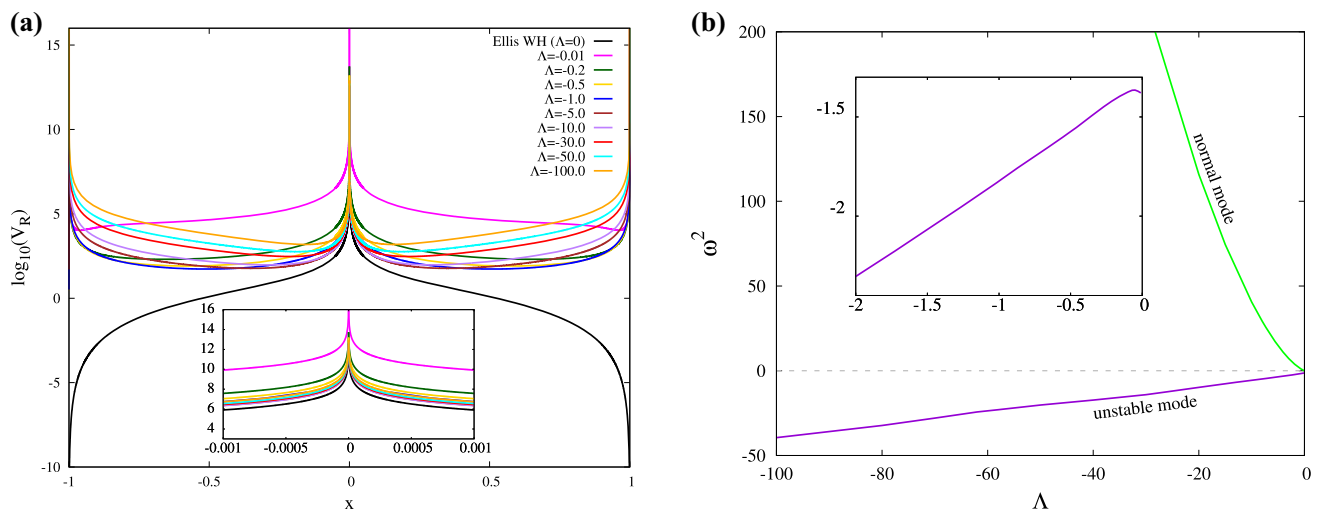
Fig. 4 **a** Radial effective potential V_R vs. compactified radial coordinate x for several values of Λ; **b** eigenvalue ω^2 of the unstable mode vs. Λ

5 Conclusion and outlook

We have numerically constructed the globally regular solutions of static Ellis wormholes with AdS asymptotics. The wormhole solutions are symmetric with respect to $\eta \to -\eta$ and consequently massless. Our numerics indicate that these solutions exist for any value of the negative cosmological constant, although in this work we have focused the discussion on the range $-100 \le \Lambda < 0$. The AdS asymptotics of the metric is reflected in the corresponding dependence of the metric components, where the g_{tt} component behaves as $\sim \eta^2$ at spatial infinity, while $g_{\eta\eta}$ behaves as $\sim -\eta^{-2}$.

The wormholes possess a single throat which, because of the symmetry and the radial coordinate that we have used, is located at the position $\eta = 0$. By decreasing Λ, the (scaled) circumferential radius of the throat decreases monotonically, approaching zero in the limit of infinite cosmological constant. In this case the circumferential coordinate tends towards the modulus of the radial coordinate η. The wormholes violate the null energy condition, as implied by the presence of a phantom field.

In addition, we have also studied the stability of these wormholes against spherically symmetric perturbations. Using the same approach as for the asymptotically flat Ellis wormholes, we have shown that the asymptotically AdS wormholes are also unstable against radial linear perturbations. The unstable mode tends to the value of the asymptotically flat case when $\Lambda \to 0$, and it increases in magnitude as the AdS length is decreased. We have also shown the existence of normal modes, which are allowed by the box-like properties of the spacetime.

It will be interesting to construct the rotating generalizations of these new Ellis wormholes with AdS asymptotics and observe how the negative cosmological constant will affect their properties. The asymptotically flat wormholes form families of solutions that tend to an extremal Kerr black hole in the rapidly rotating limit. If asymptotically AdS wormholes show an analogous feature, they should approach extremal Kerr-AdS black holes. Moreover, it will be important to investigate the stability of these rotating asymptotically AdS wormholes to see whether rotation may possibly stabilize the solutions also in the AdS case.

Let us end with some remarks in yet another direction [76]. Recently, wormholes with AdS asymptotics have also been considered in the context of ER=EPR conjecture [77] (where EPR stands for Einstein–Podolsky–Rosen and ER for Einstein–Rosen). Such wormholes might provide an alternative to introducing nonlocal interactions between the inside and outside of the horizon [78,79] without violating known principles of quantum mechanics, in order to resolve the information loss paradox of black holes [80]. There have been numerous candidate proposals (see, e.g., [81] for a review), but many of them were not successful, and several candidates have been criticized, for example black hole complementarity [82,83] or the firewall conjecture [84]. According to the conjecture, for a given entangled particle (EPR), there exists its dual geometry as ER bridge [1]. This implies that through the ER bridge, there can exist a conspiracy between the earlier part of Hawking radiation and the inside degrees of freedom.

We expect that wormhole solutions in AdS, similar to the ones we have studied in this work, can also be constructed in more general gravity theories, in particular string-inspired models. The existence of these wormhole solutions in such models might open a new window toward the study of the information loss paradox. In these models, can the philosophy of the ER=EPR conjecture still be true? When the ER=EPR conjecture was first proposed, people assumed that the ER bridge must be non-traversable, because there

is no information transfer via EPR pairs. However, it was later noticed that the ER bridge can become traversable if one considers non-perturbative effects [85] or correlations between two asymptotic boundaries [86]. If one constructs a traversable wormhole from a well-defined dual field theory, it might be consistent with the ER=EPR conjecture. On the other hand, if a traversable wormhole can be obtained from a more classical or semiclassical construction, it may indicate that the original proposal of the ER=EPR conjecture may be inconsistent or that the proposal should be restricted. In order to do this, the violation of the averaged null energy condition would be required [87], which would be possible if one did not consider the expectation value of the energy-momentum tensor of the entire histories [85] (i.e., if one would consider only a specific non-perturbative process [84,88–90]) or if the theory would violate causality somewhat due to modifications of gravity (e.g., [35–45]).

What is the physical meaning of the violation of the causality in such a theory? Can the same method of [91] be applicable in this theory? We leave these interesting questions for future projects.

Data Availability Statement This manuscript has no associated data or the data will not be deposited. [Authors' comment: All data will be shared upon request.]

References

1. A. Einstein, N. Rosen, Phys. Rev. **48**, 73 (1935)
2. M.S. Morris, K.S. Thorne, Am. J. Phys. **56**, 395 (1988)
3. M. Visser, *Lorentzian Wormholes: From Einstein to Hawking* (AIP, Woodbury, 1995)
4. F.S. Lobo, Fundam. Theor. Phys. **189**, 1 (2017)
5. H.G. Ellis, J. Math. Phys. **14**, 104–118 (1973)
6. H.G. Ellis, Gen. Relativ. Gravity **10**, 105–123 (1979)
7. K.A. Bronnikov, Acta Phys. Polon. B **4**, 251–266 (1973)
8. R.R. Caldwell, Phys. Lett. B **545**, 23 (2002)
9. S.M. Carroll, M. Hoffman, M. Trodden, Phys. Rev. D **68**, 023509 (2003)
10. G.W. Gibbons, (2003). arXiv:hep-th/0302199
11. S. Hannestad, Int. J. Mod. Phys. A **21**, 1938 (2006)
12. K.A. Bronnikov, J.C. Fabris, Phys. Rev. Lett. **96**, 251101 (2006)
13. S. Chen, M. Wang, J. Jing, Class. Quantum Gravity **33**(19), 195002 (2016)
14. B. Kleihaus, J. Kunz, E. Radu, Phys. Lett. B **797**, 134892 (2019)
15. V. Dzhunushaliev, V. Folomeev, R. Myrzakulov, D. Singleton, JHEP **0807**, 094 (2008)
16. T. Torii, H.A. Shinkai, Phys. Rev. D **88**, 064027 (2013)
17. P.E. Kashargin, S.V. Sushkov, Gravit. Cosmol. **14**, 80 (2008)
18. P.E. Kashargin, S.V. Sushkov, Phys. Rev. D **78**, 064071 (2008)
19. B. Kleihaus, J. Kunz, Phys. Rev. D **90**, 121503 (2014)
20. X.Y. Chew, B. Kleihaus, J. Kunz, Phys. Rev. D **94**(10), 104031 (2016)
21. V. Dzhunushaliev, V. Folomeev, B. Kleihaus, J. Kunz, E. Radu, Phys. Rev. D **88**, 124028 (2013)
22. V. Dzhunushaliev, V. Folomeev, C. Hoffmann, B. Kleihaus, J. Kunz, Phys. Rev. D **90**(12), 124038 (2014)
23. C. Hoffmann, T. Ioannidou, S. Kahlen, B. Kleihaus, J. Kunz, Phys. Rev. D **95**(8), 084010 (2017)
24. C. Hoffmann, T. Ioannidou, S. Kahlen, B. Kleihaus, J. Kunz, Phys. Lett. B **778**, 161 (2018)
25. C. Hoffmann, T. Ioannidou, S. Kahlen, B. Kleihaus, J. Kunz, Phys. Rev. D **97**(12), 124019 (2018)
26. V. Dzhunushaliev, V. Folomeev, B. Kleihaus, J. Kunz, JCAP **1104**, 031 (2011)
27. V. Dzhunushaliev, V. Folomeev, B. Kleihaus, J. Kunz, Phys. Rev. D **85**, 124028 (2012)
28. V. Dzhunushaliev, V. Folomeev, B. Kleihaus, J. Kunz, Phys. Rev. D **87**(10), 104036 (2013)
29. V. Dzhunushaliev, V. Folomeev, B. Kleihaus, J. Kunz, Phys. Rev. D **89**(8), 084018 (2014)
30. A. Aringazin, V. Dzhunushaliev, V. Folomeev, B. Kleihaus, J. Kunz, JCAP **1504**(04), 005 (2015)
31. J.A. Gonzalez, F.S. Guzman, O. Sarbach, Class. Quantum Gravity **26**, 015010 (2009)
32. J.A. Gonzalez, F.S. Guzman, O. Sarbach, Class. Quantum Gravity **26**, 015011 (2009)
33. K.A. Bronnikov, R.A. Konoplya, A. Zhidenko, Phys. Rev. D **86**, 024028 (2012)
34. J. Carlos Deláguila, T. Matos, Phys. Rev. D **103**, 084033 (2021)
35. D. Hochberg, Phys. Lett. B **251**, 349–354 (1990)
36. H. Fukutaka, K. Tanaka, K. Ghoroku, Phys. Lett. B **222**, 191–194 (1989)
37. K. Ghoroku, T. Soma, Phys. Rev. D **46**, 1507–1516 (1992)
38. N. Furey, A. DeBenedictis, Class. Quantum Gravity **22**, 313–322 (2005)
39. K.A. Bronnikov, E. Elizalde, Phys. Rev. D **81**, 044032 (2010)
40. P. Kanti, B. Kleihaus, J. Kunz, Phys. Rev. Lett. **107**, 271101 (2011)
41. S.V. Sushkov, R. Korolev, Class. Quantum Gravity **29**, 085008 (2012)
42. P. Kanti, B. Kleihaus, J. Kunz, Phys. Rev. D **85**, 044007 (2012)
43. X.Y. Chew, B. Kleihaus, J. Kunz, Phys. Rev. D **97**, 064026 (2018)
44. G. Antoniou, A. Bakopoulos, P. Kanti, B. Kleihaus, J. Kunz, Phys. Rev. D **101**(2), 024033 (2020)
45. R. Ibadov, B. Kleihaus, J. Kunz, S. Murodov, Phys. Rev. D **102**(6), 064010 (2020)
46. J.L. Blázquez-Salcedo, C. Knoll, Eur. Phys. J. C **80**(2), 174 (2020)
47. J.L. Blázquez-Salcedo, C. Knoll, E. Radu, Phys. Rev. Lett. **126**(10), 101102 (2021)
48. T. Damour, S.N. Solodukhin, Phys. Rev. D **76**, 024016 (2007)

49. V. Cardoso, E. Franzin, P. Pani, Phys. Rev. Lett. **116**(17), 171101 (2016) [**Erratum: Phys. Rev. Lett. 117, no. 8, 089902 (2016)**]
50. P.G. Nedkova, V.K. Tinchev, S.S. Yazadjiev, Phys. Rev. D **88**(12), 124019 (2013)
51. G. Gyulchev, P. Nedkova, V. Tinchev, S. Yazadjiev, Eur. Phys. J. C **78**(7), 544 (2018)
52. M. Amir, A. Banerjee, S.D. Maharaj, Ann. Phys. **400**, 198 (2019)
53. F. Abe, Astrophys. J. **725**, 787 (2010)
54. Y. Toki, T. Kitamura, H. Asada, F. Abe, Astrophys. J. **740**, 121 (2011)
55. R. Takahashi, H. Asada, Astrophys. J. **768**, L16 (2013)
56. J.G. Cramer, R.L. Forward, M.S. Morris, M. Visser, G. Benford, G.A. Landis, Phys. Rev. D **51**, 3117 (1995)
57. V. Perlick, Phys. Rev. D **69**, 064017 (2004)
58. N. Tsukamoto, T. Harada, K. Yajima, Phys. Rev. D **86**, 104062 (2012)
59. C. Bambi, Phys. Rev. D **87**, 107501 (2013)
60. M. Zhou, A. Cardenas-Avendano, C. Bambi, B. Kleihaus, J. Kunz, Phys. Rev. D **94**(2), 024036 (2016)
61. E. Deligianni, J. Kunz, P. Nedkova, S. Yazadjiev, R. Zheleva, Phys. Rev. D **104**(2), 024048 (2021)
62. J.L. Blázquez-Salcedo, X.Y. Chew, J. Kunz, Phys. Rev. D **98**(4), 044035 (2018)
63. J.P.S. Lemos, F.S.N. Lobo, S. Quinet de Oliveira, Phys. Rev. D **68**, 064004 (2003)
64. R.V. Korolev, S.V. Sushkov, Phys. Rev. D **90**, 124025 (2014)
65. A. Anabalón, J. Oliva, JHEP **1904**, 106 (2019)
66. G. Franciolini, L. Hui, R. Penco, L. Santoni, E. Trincherini, JHEP **01**, 221 (2019)
67. S. Mironov, V. Rubakov, V. Volkova, Class. Quantum Gravity **36**(13), 135008 (2019)
68. A. Anabalón, B. de Wit, J. Oliva, JHEP **09**, 109 (2020)
69. M. Nozawa, Phys. Rev. D **103**(2), 024005 (2021)
70. N. Chatzifotis, G. Koutsoumpas, E. Papantonopoulos, Phys. Rev. D **104**(2), 024039 (2021)
71. E. Poisson, M. Visser, Phys. Rev. D **52**, 7318–7321 (1995)
72. U. Ascher, J. Christiansen, R.D. Russell, Math. Comput. **33**(146), 659–679 (1979)
73. A. Ashtekar, A. Magnon, Class. Quantum Gravity **1**, L39–L44 (1984)
74. A. Ashtekar, S. Das, Class. Quantum Gravity **17**, L17 (2000)
75. S. Das, R.B. Mann, JHEP **08**, 033 (2000)
76. B. Freivogel, D.A. Galante, D. Nikolakopoulou, A. Rotundo, JHEP **01**, 050 (2020)
77. J. Maldacena, L. Susskind, Fortsch. Phys. **61**, 781 (2013)
78. D. Yeom, (2016). arXiv:1601.02366 [hep-th]
79. J. Hwang, H. Park, D. Yeom, H. Zoe, J. Korean Phys. Soc. **73**(10), 1420 (2018)
80. S.W. Hawking, Phys. Rev. D **14**, 2460 (1976)
81. P. Chen, Y.C. Ong, D. Yeom, Phys. Rept. **603**, 1 (2015)
82. D. Yeom, H. Zoe, Phys. Rev. D **78**, 104008 (2008)
83. D. Yeom, H. Zoe, Int. J. Mod. Phys. A **26**, 3287 (2011)
84. P. Chen, Y.C. Ong, D.N. Page, M. Sasaki, D. Yeom, Phys. Rev. Lett. **116**(16), 161304 (2016)
85. P. Chen, C.H. Wu, D. Yeom, JCAP **1706**, 040 (2017)
86. J. Maldacena, X.L. Qi, (2018). arXiv:1804.00491 [hep-th]
87. T. Hartman, S. Kundu, A. Tajdini, JHEP **1707**, 066 (2017)
88. M. Sasaki, D. Yeom, JHEP **1412**, 155 (2014)
89. P. Chen, G. Domènech, M. Sasaki, D. Yeom, JHEP **1707**, 134 (2017)
90. P. Chen, M. Sasaki, D. Yeom, Eur. Phys. J. C **79**(7), 627 (2019)
91. A. Almheiri, R. Mahajan, J. Maldacena, Y. Zhao, JHEP **03**, 149 (2020)